1 ATOMS AND MOLECULES AS BOUND QUANTUM SYSTEMS

This book will examine and explain the scattering processes of intermediate to high energy electrons in collisions with a variety of atoms and molecules. It will cover the impact energy range from the first ionization energy of most atoms and molecules (about 10–15 eV) to energies at or above 2000 eV. Since the response of an atomic or molecular target to the incident electron depends on both its impact energy and the structural properties of the target itself, it is appropriate to begin with an overview of atoms and molecules as bound quantum systems. Historical references will therefore be pertinent in this context.

1.1 INTRODUCTION – A BRIEF HISTORY OF THE STUDY OF ELECTRON SCATTERING

The beginning of the twenty-first century should be considered as a centenary marker for a number of fundamental developments in physics. The year 2014 was the centenary of the first announcement of the famous Franck and Hertz Experiment. Conducted in 1914, the Franck–Hertz Experiment is widely regarded as the one that provided validation for the Bohr theory of atomic structure, itself published only a year back, in 1913. It should also be viewed as the first quantitative experiment in electron scattering and the birth of scientific study of atomic and molecular phenomena by collisions. The original Franck–Hertz experiment passed a beam of electrons through mercury vapour with subsequent detection of the kinetic energy of the transmitted electrons. A characteristic series of peaks were observed, separated by 4.9 eV (254 nm), precisely the energy needed to achieve the first excited state of the mercury atom (Figure 1.1). Thus an incident electron, scattered by the atom, transferred its kinetic energy to the target, resulting in exciting the atom. Measuring the energy lost by scattering electrons makes it possible to determine excitation energies in the target, and this is the basis of the now standard analytical technique of Electron Energy Loss Spectroscopy (EELS).
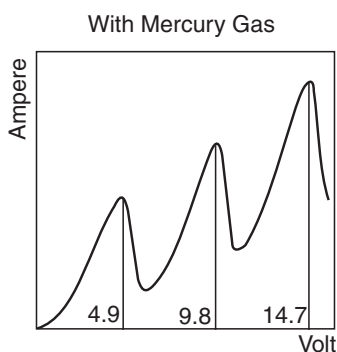
Figure 1.1   The typical Franck–Hertz electron curve showing the presence of a series of peaks separated by 4.9 eV (254 nm) characteristic of the excitation energy of the first electronic state of mercury

Once the true nature of the Franck–Hertz experiment was understood (the authors originally believing it to be an ionization phenomenon), a series of electron transmission experiments were performed. Ramsauer (1921) developed a more sophisticated apparatus using magnetic fields to collimate a beam of electrons whose energy could be more accurately defined (Figure 1.2). At low energies (less than 1 eV) when electrons passed through a chamber containing one of the heavier rare gases (Argon, Krypton, and Xenon) the gas appeared to be 'transparent' with little or no scattering occurring, even for elastic scattering (Figure 1.2b). Such a phenomenon could not be explained by any classical theory which, from its 'billiard balls approach', would lead to expectations of both significant scattering and, at lower energies, with correspondingly longer interactions times, a larger scattering cross section. However, by applying the Schrodinger equation of quantum mechanics and considering the electron projectile as an incident wave composed of partial waves characterized by the momentum of the electron, this Ramsauer–Townsend minimum (Townsend conducted similar contemporary experiments at Oxford in the UK) could be explained. Accordingly, quantum mechanics could be employed to study electron–atom/molecular interactions and calculate scattering cross sections which could be validated by experiment.

Thus it became possible to quantify electron collisions and use these cross sections to model natural and laboratory phenomena. Mott and Massey, in the UK, are considered pioneers in ushering in the era of theoretical collision physics (Mott and Massey 1965). The first applications of this theory coincided with the technological development of radar and the discovery of the ionosphere. Ionospheric models and a physical description of that most magnificent of natural phenomena, the aurora, were based on theoretical descriptions and experimental measurement of electron–atom and electron–molecule collisions leading to excitation and ionization of the target species.
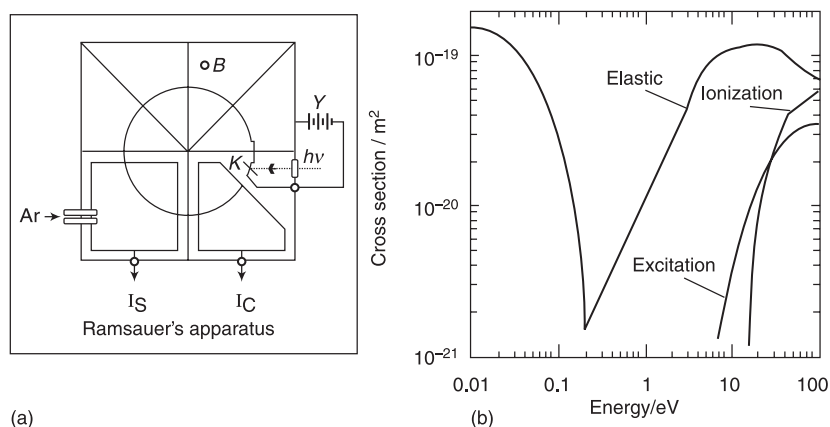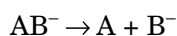
Figure 1.2   (a) The Ramsauer apparatus used to measure low energy scattering from atoms and molecules, revealing (b) the Ramsauer–Townsend minimum in the total and elastic scattering cross section of the rare gases

A major breakthrough came in the 1960s with the development of 'monochromated' electron beams, typically beams with resolution of less than 100 meV (milli electron volts), capable of resolving vibrational structure in energy loss spectra. Such high resolution electron beams also revealed unexpectedly fine structures in collision cross sections. For example, a sharp dip in the elastic scattering cross section of electrons from helium at 19.317 eV (Figure 1.3). Such a phenomenon, below the first excited state of helium (19.819 eV), appeared to have no explanation but similar effects were seen in other atoms and molecules. Schulz (1963, 1973) proposed that these 'resonances' could be explained if the electron was temporarily 'captured' by the target to form a 'temporary negative ion (TNI)' with a life of only femtoseconds or picoseconds before decaying by auto-detachment, thereby displaying Delayed Elastic Scattering, i.e.,

$$e + AB \rightarrow AB^- \rightarrow AB + e$$

An alternative route of decay leads to the fragmentation of the TNI to form an anionic product

$$AB^- \rightarrow A + B^-$$

a process known as Dissociative Electron Attachment or DEA. DEA cross sections are strongest for targets containing halogen atoms (since they are electronegative) but may be large in compounds containing 'pseudo-halogen' chemical groups such as –CN. DEA occurs naturally in the Earth's ionosphere where O^- anions are formed by DEA to molecular oxygen.
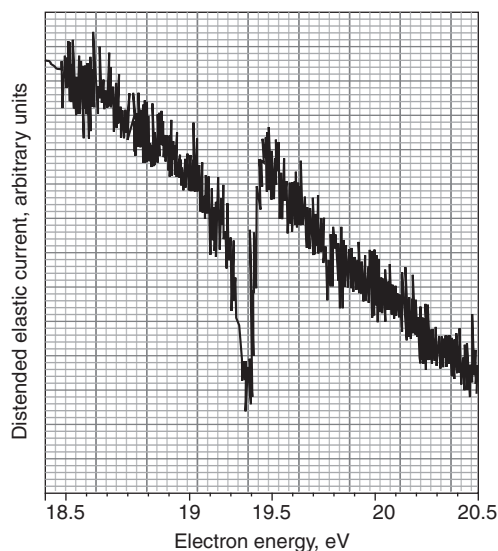
Figure 1.3   The first observation of an electron scattering resonance in helium (Schulz 1963)

The desire to understand the dynamics of electron scattering led to ever more sophisticated experiments, including the study of electron–photon coincidences (Kleinpoppen et al. 2013) to probe electron induced excitation (mainly of rare gases); electron–ion coincidence experiments (Maerk and Dunn 2010) to explore electron induced ionization and possible correlation between incident, scattered, and ejected electrons; the study of spin polarized electrons scattering from atoms and molecules (Gay 2009); and electron scattering in the presence of laser fields (Mason 1993); to couple electron scattering with photon excitation of the target. This included the study of 'electron induced' de-excitation or 'super-elastic' scattering and simultaneous electron–photon excitation. Such detailed experiments provided challenging tests of theoretical concepts about electron collisions, and required commensurate development of theory. Noteworthy progress accrued from coupling quantum mechanics based depictions of the scattering, with quantum chemistry based depictions of the target structures. Several 'formalisms' were developed and have stood the test of time with the R-matrix techniques (Burke 2011) derived from nuclear physics perhaps being the most well-known. However, there are many other methods with individual strengths and weaknesses and applicability to one scattering process or another. Carsky and Curik (2011) may be referred to for comprehensive information.

By the 1990s it was recognized that electron collisions were responsible for many diverse phenomena and thus the numbers of atomic and molecular targets to be investigated grew exponentially. For example, with the discovery of the 'ozone hole' and growth of awareness on global warming, certain molecules were identified as having 'global warming potential' and 'ozone depletion potential'. It was in this context that electron collision data was required for many molecular species that

had not previously been studied, such as ozone, and chloro- and fluorocarbons. The recognition that electrons play a crucial role in radiation damage to biological systems has led to electron studies with bio-macromolecules including DNA. Bodies in the Solar System such as the Earth, other planets and their satellites, comets, etc., are nature's wonderful laboratories where electron–atom/molecule collisions take place continuously. With the launching of various space and planetary missions, electron collision studies have found fresh relevance. The recent Cassini-Huygens mission to Saturn and its moons has revealed that Titan (considered similar to early primordial Earth) has rich ionospheric chemistry. Electron induced processes are important in the upper atmospheres of Jupiter and Saturn where aurora have been observed and there is recent interest in the atmosphere of Mars, where electron collision based ionization is known to play a role in airglow as observed by orbiting spacecraft. Similarly, the recent Rosetta mission to a comet has revealed that electron collisions play a major role in many physical and chemical processes prevalent on these intriguing celestial bodies.

Electron scattering studies are also providing useful inputs in technological fields such as gaseous electronics and electrical discharges, mass spectrometry, lasers and plasma systems, to name just a few. A technique worthy of mention is known as FEBID (Focused Electron Beam Induced Deposition) where a highly collimated beam of very high energy electrons is directed along with a feed gas onto the target substrate. This results in the formation of metallic nanostructures on the surface that are essential for latest generation electronic devices. Electron collisions are also at the core of many plasma tools including those now used in surgery and dentistry, and play an important role in plasmas that provide lighting.

It is therefore amazing to see how the poineering experiment of Franck and Hertz, just over a hundred years ago, has culminated in the application of electron scattering from so many diverse atoms and molecules in myriad applications in science and technology. The role and applications of electron scattering constitute the final chapter of this book, but meanwhile our main focus is to examine the mechanisms of electron scattering and present a detailed overview of our current knowledge of such scattering by the many atomic and molecular targets.

This book is, therefore, a systematic compilation of the studies of inter-particle *collisions,* events of rather short duration, wherein two particles interact mutually. *Scattering,* resulting from a collision, is the deflection of the incident beam or the projectile particles caused by a target system. It is customary to use the term 'collision' or 'scattering' or 'collisional interaction' interchangeably. The same applies to discourses on electron impact phenomena or processes. Here, we examine the resulting change in the states of the scattering systems, i.e., see what happens to both the colliding electron and the target atom or molecule. As such, we follow the footsteps of many eminent scientists and their works, such as the earliest treatises, namely, *Theory of Atomic Collisions,* by Mott and Massey (1965), and well-known books written by Bransden and Joachain (2003), Joachain (1983), and Khare (2001).

At the very beginning of any study of electron scattering, it is appropriate to view an atom (or a molecule) as a quantum mechanically bound system composed of electrons and nucleus (or nuclei). A brief survey of atomic and molecular structure properties is therefore necessary in order to develop a basic understanding of the targets for electron scattering. Hydrogen and helium atoms are dealt with in some detail, while other atoms and molecules have been given briefer treatment.

1.2   THE HYDROGEN ATOM AND MULTI-ELECTRON ATOMS

A one-electron system like the hydrogen atom is an exactly solvable problem in quantum mechanics (Bransden and Joachain 2003). The corresponding energy eigenvalues and eigenfunctions are derived from the analytical solution of the time-independent Schrödinger equation,

$$\left[\frac{-\hbar^2 \nabla^2}{2m} - \frac{Ze^2}{4\pi\varepsilon_0 r} \right] \psi(r) = E\,\psi(r) \tag{1.1}$$

In this equation, $\boldsymbol{r}$ (with $r = |\boldsymbol{r}|$) is the radial coordinate of the electron (having mass m) with reference to the proton (nucleus), ∇^2 is the Laplacian operator and Z is the atomic number. The total energy of the system is E and $\psi(\boldsymbol{r}) = \psi_{n\ell m}(r, \theta, \varphi)$ is the stationary wave function of the atomic electron. The principal quantum number is represented by n, the orbital angular momentum quantum number by ℓ, and the corresponding projection quantum number by m_ℓ or simply m. These quantum numbers have the standard discrete values. (Please see also Box 1.1). In the case of the hydrogen atom, the energy eigenvalues E_n derived from equation (1.1) can be expressed by the exact formula

$$E_n = -\frac{13.6}{n^2}\,\text{eV} \tag{1.2}$$

The energy level diagram of the hydrogen atom, generated from equation (1.2), is shown in Figure 1.4.

The ground state wave function of this atom written as $\psi_{100}(\text{r})$ or ψ_{1s}, also referred to as the 1s orbital, is

$$\psi_{1s}(r) = \frac{1}{\sqrt{(\pi a_0^3)}} \exp\left(-\frac{r}{a_0} \right) \tag{1.3}$$

From equation (1.3) one finds that in this case the electron charge density is $\rho(r) = e\,|\psi_{1s}(r)|^2$ and this gives us the radial charge density $D(r) = 4\pi r^2 \rho(r)$, a quantity that peaks at the first Bohr radius a_0, which is a typical length on the atomic scale (Box 1.1). There are a few important observations on the H atom.

- There is a large energy difference between the ground state $n = 1$(1s) and the first excited states $n = 2$ (2s, 2p), but the energy levels get closer together as n increases.
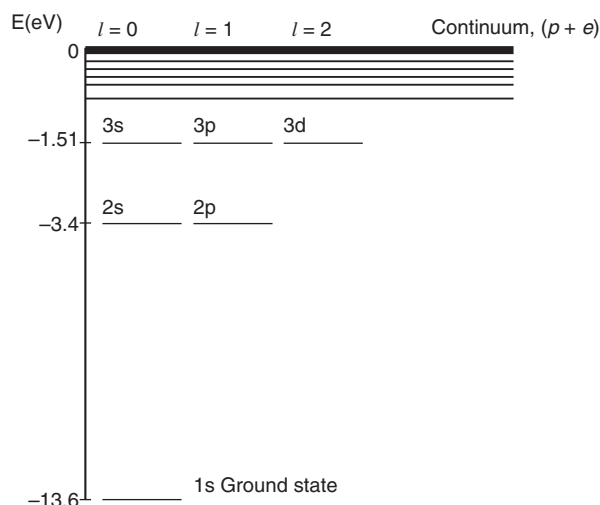
Figure 1.4   Energy levels of the Hydrogen atom, from equation (1.2)

BOX 1.1: ATOMIC UNITS (au) AND SYMBOLS

Standard symbols are used, as follows:

$\hbar = h/2\pi$, with h = Planck's constant; m_e = electron rest-mass (symbol 'm' is also used, not to be confused with the projection quantum number m); e = electron charge; ε_0 = free-space permittivity;

Å stands for the Angstrom unit of length, 1 Å = 10^{-10} m; and

a_0 = the usual first Bohr radius of the H(1s) atom = 0.529×10^{-10} m = 0.529 Å.

In the atomic-molecular regime atomic units (au in short) are defined by assuming $\hbar = m_e = e = 1$, also $4\pi\varepsilon_0 = 1$. Thus in atomic units, the Bohr radius, $a_0 = 1$ and is taken as a unit of length. In au the two units of energy adopted are the Rydberg (R) and the Hartree with 1 R= 13.6 eV, the ground-state ionization energy of atomic hydrogen, while 1 Hartree = 2 R = 27.2 eV. 1 electron Volt (eV)=1.602×10^{-19} J.

For an electron in an atom the usual quantum numbers n, ℓ, and m_ℓ have been defined in preceding text. We have the principal quantum number n = 1,2,3,4 ... corresponding to shells K, L, M, N, etc., while ℓ = 0, 1, 2, 3....(n – 1) are referred to by code letters s, p, d, f, etc. For each ℓ, the projection quantum number m_ℓ admits ($2\ell + 1$) values from $+\ell$ to $-\ell$, including zero. For an atom with number of electrons N ≥ 2, the quantum number for electronic total orbital angular momentum admits values L = 0, 1, 2, 3, ... etc., and the corresponding states are denoted by upper case letters *S, P, D, F,* ..... etc. Thus the ground state of the two-electron atom like helium is denoted by $^1S_0$, where the left superscript '1' stands for total spin singlet state, while the right subscript '0' indicates the total angular momentum quantum number J = L + S = 0.

- The ground state (also called first) ionization energy is I_{1s} = 13.6 eV but the ionization energy is only 3.4 eV for n = 2 (Figure 1.4). There are infinitely many discrete excited states of atomic hydrogen between the first excited state and the ground-state ionization potential. The dipole selection rule governing transitions in the 1-electron atom states that, if the ℓ-value changes by 1, i.e., if $\Delta\ell = \pm 1$, then the transition is dipole allowed. This also implies the change in parity of the system wave function. Thus, the transition 1s $\leftrightarrow$ 2p is dipole allowed and the radiative life time of the 2p state is typically $\tau(2p) \sim 10^{-9}$ s. H atoms in 2p state emit the famous Lyman - α line with a wavelength of about 121.3 nm or a photon energy close to 10.2 eV. In contrast, the transition 1s $\leftrightarrow$ 2s is forbidden and hence the H-atom in 2s state is metastable with a very large radiative lifetime $\tau(2s)$ of about 1/7s. This has important consequences as the excited metastable atom can act as an energy store in the embedding medium. For transitions induced by incident electrons there are no selection rules and therefore an electron can excite the ground state of the atom to a metastable state.

- Highly excited states or high 'n' states ($n \sim 100$) are known as Rydberg states and they can exist in certain astrophysical systems.

- Transition probabilities from the ground state to different excited states, expressed in terms of oscillator strengths, have been discussed in advanced textbooks on this subject (e.g., Bransden and Joachain 2003). It should be noted that for atomic hydrogen the continuum oscillator strength is close to the sum of oscillator strengths of all discrete transitions, and the latter are clearly dominated by the final state n = 2.

- The continuous positive energy regime or continuum (Figure 1.4) corresponds to a system of a free proton (nucleus) and a free electron. So how do we know whether a free proton and a free electron coming closer together form a bound system, i.e., a H atom, or would they just scatter apart from one another? The answer depends on the total energy of the system. In a bound state the total energy is negative while in scatterable (free) states it remains positive at any separation.

An important result, giving us an idea of the size of the H atom, is the exact expectation (or the quantum mechanical average) value of the 'radius' <r> in a given state. For the ground state this is,

$$\langle r \rangle_{\mathrm{H}} = 1.5\, a_0 \tag{1.4}$$

Now consider the helium atom for which a detailed quantum mechanical treatment may be found in standard texts. Although the Schrödinger equation in this case does not yield an exact analytical solution, very accurate eigen functions and eigen values have been determined.

Some important points to note:

- Similar to the hydrogen atom the first two excited states of helium - denoted by 2^3S and 2^1S – have large excitation energies, while subsequent states are closer and closer together. The singly excited states of He, up to the first ionization threshold at I_{He} = 24.6 eV, are bunched within in an energy span of about 5 eV.

- The excited states 2^3S and 2^1S are metastable with large radiative lifetimes.

- The first ionization threshold of helium at 24.6 eV is the largest of any atom in the periodic table.

As per the scope of this book, suffice it to state that theoretical methods or structure calculations for atoms with atomic number $Z \geq 3$ began with the development of Hartree-Fock and Thomas–Fermi methods in the 1930s and currently may be calculated using commercial software package. Notable indeed was the work of Cox and Bonham (1967), who developed methods for determining the atomic electron charge density and static potential for atoms up to $Z = 54$ in parametric forms. Roothan–Hartree–Fock wave functions were presented analytically by Clementi and Roetti (1974) and were extended for heavier atoms with $Z = 55$–92 by (McLean and McLean 1981). Later improvements were made by Bunge and associates in 1993, and Koga and others in 1995.

1.3 ATOMIC PROPERTIES – ATOMIC RADII

Some of the well-known properties of atoms that we shall be exploring in this book are: the first ionization energy I; the average radius *<r>*; and the static electric dipole polarizability α_d measured as a volume quantity. In the case of the ground-state hydrogen atom, the values for I and *<r>* are as already stated. For H-atom, α_d was obtained through a perturbation calculation (Schiff 1968) and is $\alpha_d = 9/2.a_0^3$ or 0.66 Å³. One of the most accurately known properties of atoms is ionization threshold I, which shows systematic periodic variations as a function of Z, over the entire periodic table (Bransden and Joachain 2003). For hydrogen (or 1-electron) atom, one can combine equation (1.2) with the axiom that *<r>* ~ n², to derive the dependence of I on the average radius as I ~ 1/*<r>*. Assuming the polarizability α_d ~ *<r>*³, we arrive at a simple but useful conclusion,

$$\alpha_d \sim 1/I^3$$

Such a variation of the atomic polarizability with an inverse power of I has been discussed by several authors (Fricke 1986; Politzer et al. 1991; Dmitrieva and Plindov1983; Bhowmik et al. 2011). In order to test this relationship we have considered the inert gases and the halogen atoms in Figure 1.5. We have used atomic polarizabilities α_d available from the NIST Computational Chemistry Comparison and Benchmark Data Base (or the CCCBDB in short) and from Schwerdtfeger (2015). The plots of α_d versus $1/I^3$ are fairly linear with a very good correlation coefficient R^2. A good linear correlation is also observed for halogen atoms (Figure 1.5).
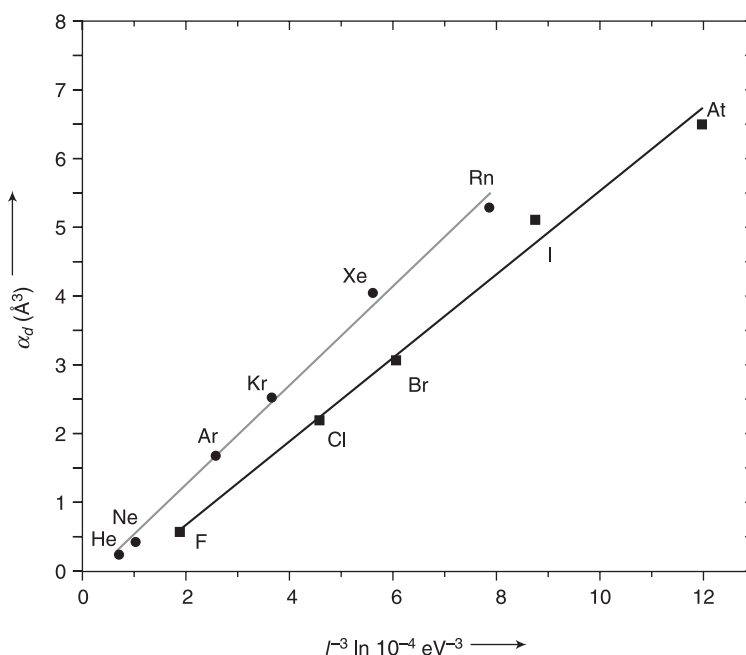
Figure 1.5   Linear correlation of α_d against $1/I^3$ for the inert-gas atoms and halogens with correlation coefficient $R^2 = 0.99446$ and 0.98975 respectively

A major focus is the *atomic/molecular scattering cross section* which is a dynamic, i.e., an energy dependent, area quantity. Therefore, it is necessary to introduce an elementary notion of *area* of an atom. The spatial extent of an atom can be gauged by defining its radius.

Quantum mechanics leads to the postulation of two types of radii. The orbital (or peak) radius 'r_p' is the radial distance from the nucleus to the peak position of the outermost orbital of electrons in the atom, while the average radius $<r>$ is the corresponding quantum mechanical expection value (Clementi and Roetti 1974; Bunge et al. 1993; Joshipura 2013). The Van der Waals radius R_W of two interacting identical atoms is defined to be the distance at which their inter-atomic attractive force turns repulsive. The fourth definition of radius comes from the response of the atom to an external electric field. Recall that the atomic electric dipole polarizability α_d is measured in volume terms. The polarizability radius is therefore defined as $R_{pol} = (\alpha_d)^{1/3}$ (Ganguly 2008). All the four types of radii of atoms are known across the entire periodic table, and the interesting behaviour of the atomic radii is shown in Figure 1.6, adopted from (Joshipura 2013; and references therein). The radii R_W and R_{pol} are shown here for inert gas atoms and alkali atoms only. For the helium atom the values (in Å) are: $r_p = 0.36$, $<r> = 0.49$, $R_{pol} = 0.59$ and $R_W = 1.4$.